Journal of Molecular and Cellular Cardiology 108 (2017) 86–94

Contents lists available at ScienceDirect

Journal of Molecular and Cellular Cardiology

journal homepage: www.elsevier.com/locate/yjmcc

Impaired mitophagy facilitates mitochondrial damage in Danon disease

Sherin I. Hashem [a], Anne N. Murphy [b], Ajit S. Divakaruni [b], Matthew L. Klos [c], Bradley C. Nelson [a], Emily C. Gault [a], Teisha J. Rowland [d], Cynthia N. Perry [a], Yusu Gu [a], Nancy D. Dalton [a], William H. Bradford [a], Eric J. Devaney [c], Kirk L. Peterson [a], Kenneth L. Jones [e], Matthew R.G. Taylor [d], Ju Chen [a], Neil C. Chi [a,f], Eric D. Adler [a,*]

[a] Department of Medicine, Division of Cardiology, University of California San Diego, La Jolla, CA, USA
[b] Department of Pharmacology, University of California San Diego, La Jolla, CA, USA
[c] Department of Surgery, University of California San Diego, La Jolla, CA, USA
[d] Cardiovascular Institute, Adult Medical Genetics Program, University of Colorado Denver, Aurora, CO, USA
[e] Department of Pediatrics, Section of Hematology, Oncology, and Bone Marrow Transplant, University of Colorado Denver, Aurora, CO, USA
[f] Institute for Genomic Medicine, University of California San Diego, La Jolla, CA, USA

ARTICLE INFO

Article history:
Received 19 April 2017
Received in revised form 14 May 2017
Accepted 15 May 2017
Available online 16 May 2017

Keywords:
Autophagy
hiPSC
Mitochondria
Cardiomyocyte
Heart failure

ABSTRACT

Rationale: Lysosomal associated membrane protein type-2 (LAMP-2) is a highly conserved, ubiquitous protein that is critical for autophagic flux. Loss of function mutations in the *LAMP-2* gene cause Danon disease, a rare X-linked disorder characterized by developmental delay, skeletal muscle weakness, and severe cardiomyopathy. We previously found that human induced pluripotent stem cell-derived cardiomyocytes (hiPSC-CMs) from Danon patients exhibited significant mitochondrial oxidative stress and apoptosis. Understanding how loss of LAMP-2 expression leads to cardiomyocyte dysfunction and heart failure has important implications for the treatment of Danon disease as well as a variety of other cardiac disorders associated with impaired autophagy.
Objective: Elucidate the pathophysiology of cardiac dysfunction in Danon disease.
Methods and results: We created hiPSCs from two patients with Danon disease and differentiated those cells into hiPSC-CMs using well-established protocols. Danon hiPSC-CMs demonstrated an accumulation of damaged mitochondria, disrupted mitophagic flux, depressed mitochondrial respiratory capacity, and abnormal gene expression of key mitochondrial pathways. Restoring the expression of *LAMP-2B*, the most abundant *LAMP-2* isoform in the heart, rescued mitophagic flux as well as mitochondrial health and bioenergetics. To confirm our findings *in vivo*, we evaluated *Lamp-2* knockout (KO) mice. Impaired autophagic flux was noted in the *Lamp-2* KO mice compared to WT reporter mice, as well as an increased number of abnormal mitochondria, evidence of incomplete mitophagy, and impaired mitochondrial respiration. Physiologically, *Lamp-2* KO mice demonstrated early features of contractile dysfunction without overt heart failure, indicating that the metabolic abnormalities associated with Danon disease precede the development of end-stage disease and are not merely part of the secondary changes associated with heart failure.
Conclusions: Incomplete mitophagic flux and mitochondrial dysfunction are noted in both *in vitro* and *in vivo* models of Danon disease, and proceed overt cardiac contractile dysfunction. This suggests that impaired mitochondrial clearance may be central to the pathogenesis of disease and a potential target for therapeutic intervention.

1. Introduction

Danon disease is a lethal X-linked disorder associated with developmental delay and profound skeletal and cardiac myopathies [1,2]. Though frequently asymptomatic in early childhood, Danon patients typically die in the second or third decade of life from progressive heart failure without heart transplantation [1,2]. The pathologic hallmark of Danon disease is the accumulation of immature autophagic vacuoles (AVs), predominantly in cardiac and skeletal muscle [1–3]. The disease is associated with an impairment in autophagy, a ubiquitous catabolic process through which dysfunctional organelles and cellular constituents are sequestered in AVs and delivered to the lysosomes for degradation and recycling [4,5].

Danon disease has been attributed to mutations in the gene encoding lysosomal associated membrane protein 2 (LAMP-2), a lysosomal membrane-bound protein that is expressed as three different isoforms (A, B, and C) generated by alternative splicing [6]. The LAMP-2B isoform is thought to play a key role in the macroautophagy pathway

* Corresponding author at: 9500 Gilman Drive, Biomedical Research Facility, Room 1217 AA, La Jolla, CA 92093, USA.
E-mail address: eradler@ucsd.edu (E.D. Adler).

http://dx.doi.org/10.1016/j.yjmcc.2017.05.007
0022-2828/

by facilitating autophagosome-lysosome fusion and is the most highly expressed isoform in the heart [6]. Mutations affecting only the expression of *LAMP-2B* have been shown to cause Danon disease [3], implicating the importance of macroautophagy (abbreviated hereafter as autophagy), in particular, in the pathogenesis of the disease.

While LAMP-2 deficiency has been studied in multiple organ systems, the specific mechanisms by which loss of LAMP-2 expression leads to cardiac dysfunction are poorly understood. As there are currently no FDA-approved therapies for treating Danon disease, death or cardiac transplantation are inevitable for most patients. Understanding how LAMP-2 deficiency results in cardiac remodeling and end-stage cardiomyopathy will provide critical insights for the development of targeted therapeutic interventions. Increasing evidence also suggests that impaired autophagy is associated with a wide spectrum of cardiovascular conditions, including a variety of inherited metabolic disorders as well as chemotherapy-induced heart failure [7–9]. Therefore, developing a better mechanistic understanding of the relationship between autophagic flux and cardiomyocyte physiology has significant therapeutic implications beyond the treatment of Danon disease.

We previously reported that human induced pluripotent stem cell-derived cardiomyocytes (hiPSC-CMs) generated from patients with *LAMP-2* mutations recapitulate key features of the failing heart *in vitro* and provide an invaluable system for studying Danon disease in human cardiac myocytes [10]. Danon hiPSC-CMs were also noted to have structurally abnormal mitochondria. Therefore, we chose to determine both the origins and ramifications of these abnormal mitochondria, using Danon hiPSC-CMs as well as a *Lamp-2* knockout (KO) mouse model of Danon disease [11].

2. Materials and methods

An expanded Materials and Methods section is available in the Online Data Supplement. Briefly, wild-type (WT) and Danon patient-derived hiPSCs were differentiated toward the cardiac myocyte lineage using a well-established protocol [12] to obtain the highest efficiency of cardiac differentiation as we previously reported [10]. We used hiPSC-CMs and a *Lamp-2* KO mouse model [11] to assess mitochondrial health, morphology, clearance, and function as previously described [10,13,14].

3. Results

3.1. Danon hiPSC-CMs exhibit significant mitochondrial damage and impaired mitophagic clearance of damaged mitochondria

To investigate the pathogenesis of Danon disease *in vitro*, we utilized hiPSCs generated from two unrelated individuals with different mutations in *LAMP-2* and a clinical diagnosis of Danon disease (Danon A and Danon B hiPSC lines) to generate cardiomyocytes as previously described [10]. Genomic sequencing of Danon A and Danon B cells revealed a 2-bp insertion in exon 2 of the LAMP-2 gene (129–130 insAT) and a single point mutation in intron 1 of the LAMP-2 gene (IVS-1 c.64 + 1 G > A), respectively [10]. These hiPSC lines had normal karyotypes and met pluripotency criteria and neither line expressed any LAMP-2 [10]. Having observed increased mitochondrial oxidative stress in Danon hiPSC-CMs in our earlier work [10], we hypothesized that the absence of LAMP-2 would interrupt the mitophagy pathway leading to the accumulation of damaged 'leaky' mitochondria which may be the source of increased reactive oxygen species (ROS) in Danon hiPSC-CMs. To explore this hypothesis, we performed immunohistochemical studies to assess the expression of the key regulators of the mitophagy pathway, PARKIN and p62, in Danon hiPSC-CMs compared to WT hiPSC-CMs. PARKIN and p62 are known to be recruited on the membranes of damaged mitochondria, marking them for clearance by mitophagy [14–17]. We noted that there was increased perinuclear clustering of damaged mitochondria exhibiting the co-localization of PARKIN and p62 with mitochondrial membrane proteins (COX IV and TOMM20) in Danon hiPSC-CMs compared to WT, suggesting the increased presence of damaged mitochondria in Danon hiPSC-CMs and that the initiation of mitophagy had been upregulated in response to compromised mitochondrial health in these cells (Fig. 1A–D, K, L). Furthermore, Danon hiPSC-CMs exhibited the presence of more depolarized mitochondria compared to WT hiPSC-CMs (Fig. 1G, H, Fig. 3E, Supplemental Fig. 1) confirming compromised mitochondrial health in Danon hiPSC-CMs compared to WT hiPSC-CMs. However, WT hiPSC-CMs (Fig. 1E) showed co-localization of mitochondria with late autolysosomes (LAMP-1-positive vesicles) more readily than Danon hiPSC-CMs (Fig. 1F), providing evidence that the transfer of dysfunctional mitochondria to lysosomes for degradation was disrupted in Danon hiPSC-CMs despite the increased mitochondrial damage (Fig.1A–H, K, L, Supplemental Fig. 1) and upregulation of mitophagy initiation. This finding was further confirmed by electron microscopy (EM) where Danon hiPSC-CMs demonstrated the accumulation of abnormal mitochondria (fragmented, swollen, or decreased cristae density) (Fig. 1M) and an increased presence of mitochondria contained within double membrane autophagosomes compared to WT controls (Fig. 1I, J, Fig. 3B, C), confirming an impairment in the trafficking of dysfunctional mitochondria from autophagosomes to lysosomes. RNA Sequencing (RNA-Seq) performed using WT and Danon hiPSC-CMs revealed significant differences in mitochondrial gene expression. Specifically, statistical analysis was used to generate a list of the most differentially expressed genes ($p \le 0.05$ and $Q \le 0.05$, 2169 genes total) and analysis of this list by Ingenuity Pathway Analysis (IPA) software reported the top three differentially expressed canonical pathways to be Oxidative Phosphorylation ($p = 5.0 \times 10^{-37}$), Mitochondrial Dysfunction ($p = 3.2 \times 10^{-35}$), and TCA Cycle II (Eukaryotic) ($p = 6.3 \times 10^{-10}$) (Supplemental Fig. 2A). Furthermore, the expression profile of genes involved in the citric acid cycle (Supplemental Fig. 2B) and oxidative phosphorylation (Supplemental Fig. 2C) were significantly upregulated in Danon hiPSC-CMs compared to WT hiPSC-CMs, further confirming the compromised mitochondrial health in LAMP-2 deficient cardiomyocytes. Taken together, this data suggests that LAMP-2 deficiency disrupts the completion of proper mitophagic flux in Danon hiPSC-CMs, impairing the ability of cells to clear damaged mitochondria.

3.2. LAMP-2 deficiency is associated with mitochondrial respiratory dysfunction in hiPSC-CMs

Given the mitophagic abnormalities we observed in Danon hiPSC-CMs (Fig. 1), we then assessed mitochondrial respiratory function in these cells using a Seahorse XF96 extracellular flux analyzer in DMEM supplemented with glucose, pyruvate, and glutamine. Danon hiPSC-CMs exhibited depressed basal and ATP-linked oxygen consumption rates (OCR) compared to WT hiPSC-CM controls (Fig. 2A, B). ATP-linked respiration is the rate of oxygen consumption dedicated to the synthesis of ATP derived from the basal rate and the rate following the addition of the ATP synthase inhibitor, oligomycin [13]. This data indicates that Danon hiPSC-CMs are producing ATP at a lower rate than WT hiPSC-CMs. Further, maximal uncoupler-stimulated respiratory capacity (a measure of the maximal rate of electron transport chain activity and oxidative metabolism) was measured with successive additions of carbonyl cyanide-4-(trifluoromethoxy) phenylhydrazone (FCCP), and was also found to be severely impaired in Danon hiPSC-CMs (Fig. 2A, B). Significant metabolic abnormalities were not evident in Danon primary fibroblasts (Fig. 2B), an observation that is consistent with the muscle-selective phenotype of this disorder and may explain why Danon disease preferentially affects metabolically active tissues. When hiPSC-CMs were permeabilized and the mitochondria were provided pyruvate or the fatty acid-derivative palmitoyl carnitine to identify specific metabolic sites of dysfunction, Danon hiPSC-CMs showed lower maximal respiratory capacity than WT hiPSC-CMs on either substrate (Fig. 2C). This data suggests that oxidation of multiple metabolic fuels are

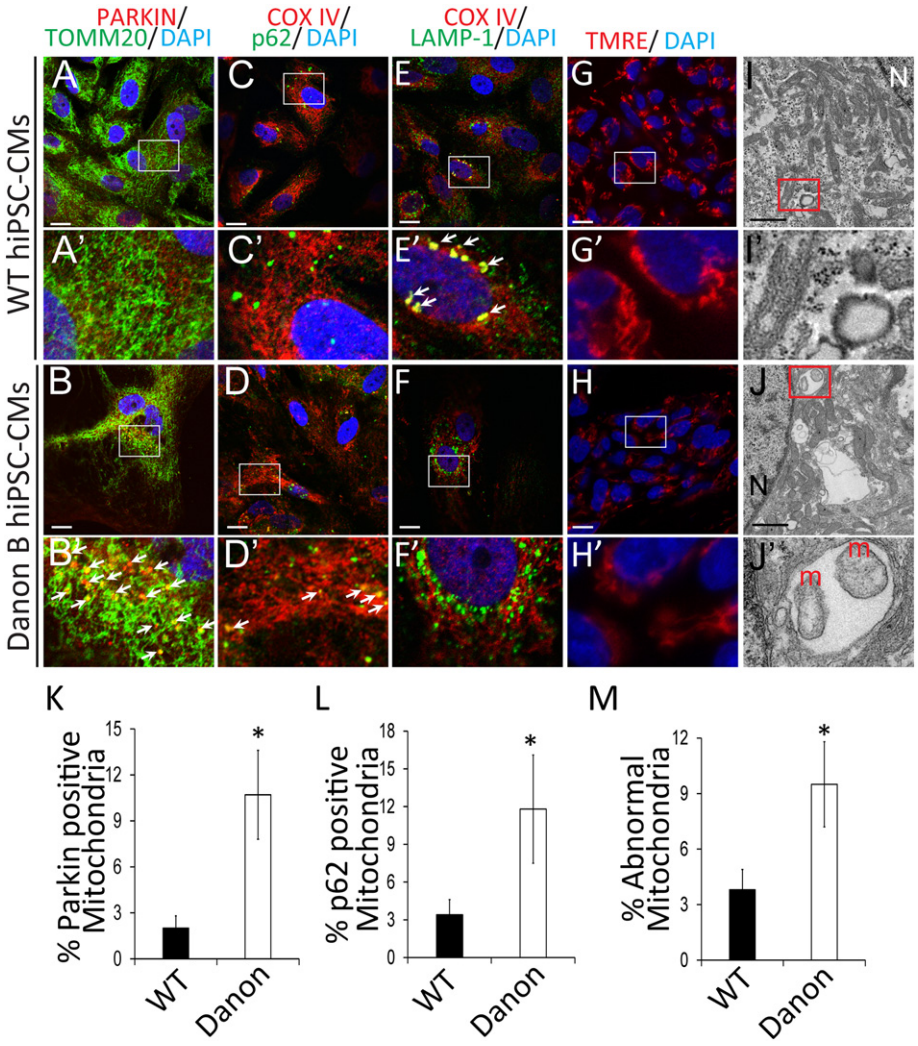

Fig. 1. Mitochondrial abnormalities and incomplete mitophagy in Danon hiPSC-CMs. (A, B) Representative confocal images of WT (A) and Danon (B) hiPSC-CMs demonstrate marked co-localization (white arrows) of PARKIN (red) with the mitochondrial membrane (TOMM20, green) in Danon hiPSC-CMs as compared to WT hiPSC-CMs. (C, D) Representative confocal images of WT (C) and Danon (D) hiPSC-CMs demonstrate marked co-localization (white arrows) of p62 (green) with the mitochondrial membrane (COX IV, red) in Danon hiPSC-CMs as compared to WT hiPSC-CMs. (E, F) Representative confocal images of WT (E) and Danon (F) hiPSC-CMs demonstrate decreased co-localization (white arrows) of LAMP-1 lysosomes (green) and mitochondria (COX IV, red) in Danon hiPSC-CMs as compared to WT hiPSC-CMs. (G, H) Representative confocal images of WT (G) and Danon (H) hiPSC-CMs demonstrate the presence of brighter TMRE-stained mitochondria in WT compared to Danon hiPSC-CMs. DAPI (blue) was used to counterstain nuclei in A–H. Scale bar = 10 μm in A–H. (I, J) Representative electron microscope (EM) images of WT (I) and Danon (J) hiPSC-CMs reveal increased presence of intact mitochondria within autophagic vacuoles (AVs) in Danon hiPSC-CMs compared to WT hiPSC-CMs. M: mitochondria; N: nucleus. Scale bar = 0.5 μm in I, J. (A′–J′) Enlarged images of boxed area in A–J. (K–M) Quantification of percentage of PARKIN-positive mitochondria assessed by immunofluorescent staining (K), percentage of p62-positive mitochondria assessed by immunofluorescent staining (L), and percentage of abnormal (fragmented, swollen, decreased cristae) mitochondria assessed by EM (M), in WT and Danon hiPSC-CMs. Student's *t*-test, n = 3–5, $^{*}p < 0.05$.

impacted by the defect, potentially at the level of the electron transport chain. Taken together, this data suggests that LAMP-2 deficiency results in the accumulation of damaged mitochondria with depressed respiratory functions.

3.3. Mitophagy and mitochondrial function are restored by re-introduction of LAMP-2B

We previously reported that overexpression of *LAMP-2B*, the isoform with the greatest role in macroautophagy and highest expression in the heart, in Danon hiPSC-CMs using a doxycycline-inducible promoter and a lentiviral delivery system (*LAMP-2B* overexpression line: *LAMP-2* OE) rescued autophagic flux, decreased mitochondrial oxidative stress and apoptotic cell death, and restored normal mitochondrial morphology [10]. Here, we used this *LAMP-2* OE hiPSC-CM line as previously described [10] to restore LAMP-2 expression in Danon hiPSC-CMs (Fig. 3A) and assess the effect of re-introducing *LAMP-2B* on mitophagic flux (Fig. 3B, C) and mitochondrial function (Fig. 3D) and health (Fig. 3E). We found that *LAMP-2B* overexpression rescued mitophagic flux, as evidenced by a decrease in the percentage of mitochondria observed within double-membraned AVs by EM (Fig. 3B, C), improved mitochondrial bioenergetics as assessed by respiration (Fig. 3D), and rescued mitochondrial health as noted by an increase in mitochondrial membrane potential (Fig. 3E), in *LAMP-2* OE hiPSC-CMs compared to Danon hiPSC-CMs. The ability of isolated *LAMP-2B* replacement to rescue mitophagy as well as mitochondrial health and function confirms that impaired macroautophagy is responsible for the mitochondrial abnormalities observed in Danon hiPSC-CMs.

3.4. Autophagic flux is impaired in Lamp-2 KO mouse hearts

To ensure that our *in vitro* findings were not a consequence of cell culture conditions, we performed further experiments using a *Lamp-2* KO murine model of Danon disease [11]. First, we sought to determine if autophagy was also impaired in *Lamp-2* KO mice. To do this, we generated a novel mouse model by crossing *Lamp-2* KO mice with a

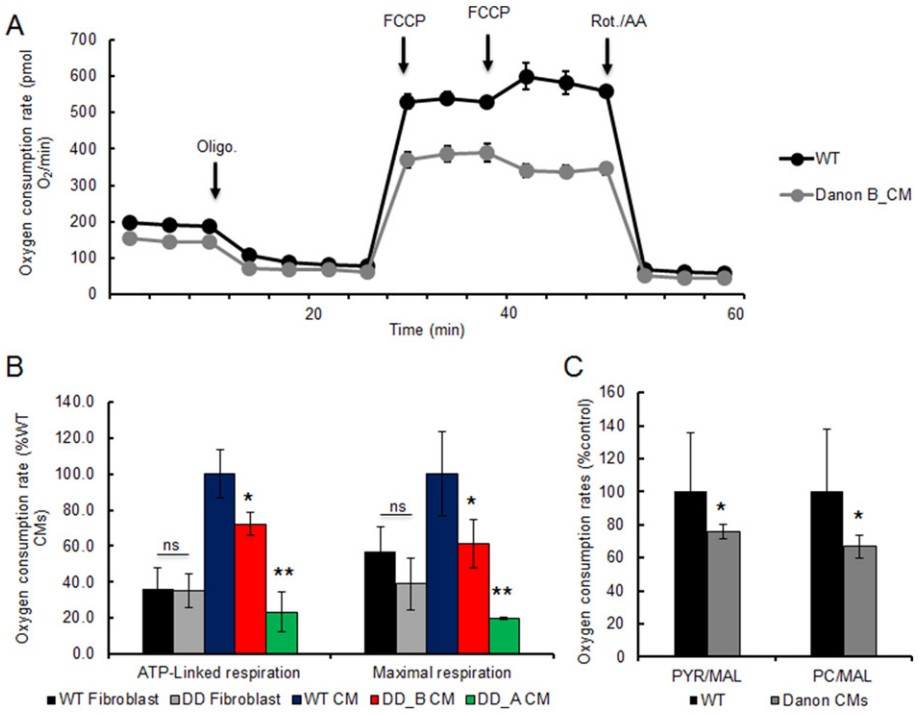

Fig. 2. Impaired cellular bioenergetics is evident in Danon hiPSC-CMs. (A–C) Mitochondrial function of Danon and WT hiPSC-CMs as assessed by the cellular oxygen consumption rate (OCR), normalized to nuclear content as measured by Hoechst stain. Representative time course data (A) and aggregate data (B, C) for n = 4–8 independent experiments using at least 5 biologic replicates. (A) Graphical representation of OCR measurement in intact WT and Danon hiPSC-CM lines with sequential additions of oligomycin (oligo), two successive additions of carbonyl cyanide-4-(trifluoromethoxy) phenylhydrazone (FCCP), followed by rotenone plus antimycin A (Rot./AA). (B) Mean OCR in intact cells reveal no difference in rates of ATP-linked oxygen consumption between WT and Danon disease (DD) fibroblast lines (OCR in pMoles O_2/min: 121.6 ± 54.4 for WT *vs.* 133.1 ± 59.6 for Danon fibroblasts). Danon hiPSC-CM lines exhibit significant depression of ATP-linked respiratory rates compared to WT hiPSC-CMs (OCR in pMoles O_2/min: 286.4 ± 64.9 for WT *vs.* 160.3 ± 22.7 for Danon A lines (DD_A CM) and 168.9 ± 22.7 for Danon B line (DD_B CM)). A similar pattern was observed in maximal rates of respiration induced with FCCP. (C) Mean OCR as a percent of the maximal uncoupler-stimulated rate in permeabilized WT cells reveal decreased OCR in Danon hiPSC-CMs compared to WT hiPSC-CMs in the presence of pyruvate plus malate (Pyr/Mal), or palmitoyl carnitine plus malate (PC/Mal) as oxidizable substrates, suggests a global loss of mitochondrial respiratory capacity (OCR in pMoles/min: 374.9 ± 76.6 and 123.2 ± 10.2 for WT *vs.* 248.1 ± 109.5 and 68.13 ± 21.2 for Danon hiPSC-CMs in the presence of pyruvate/malate or palmitoyl carnitine/malate, respectively). Two-way ANOVA with non-parametric correction followed by post-hoc Dunnett's test, $^{*}p < 0.05$, $^{**}p < 0.01$ *vs.* WT hiPSC-CMs. ns = not significant.

previously established *CAG-RFP-EGFP-LC3B* reporter line [18]. In this reporter line, early autophagosomes (not fused with lysosomes) exhibit both RFP and GFP fluorescence while late autolysosomes (following fusion of autophagosomes with lysosomes) demonstrate only RFP fluorescence as GFP is quenched by the acidic environment of the lysosomes (Fig. 4A). *Lamp-2* KO/*CAG-RFP-EGFP-LC3B* cardiomyocytes exhibited an accumulation of early autophagosomes (RFP + EGFP, yellow puncta) and were almost devoid of late autolysosomes (RFP, red puncta), confirming a failure in autophagosome-lysosome fusion in *Lamp-2* KO mice (Fig. 4B–H).

3.5. Lamp-2 KO mouse hearts exhibit accumulation of damaged mitochondria and impaired mitophagic flux

To assess the effect of LAMP-2 deficiency on mitochondria *in vivo*, we used EM to evaluate mitochondrial morphology in the hearts of *Lamp-2* KO mice and WT littermate controls at 22 weeks of age. We found that *Lamp-2* KO cardiomyocytes contained extensive clusters of AVs (Fig. 5A, B, F) that were considerably larger in size than those seen in WT littermate controls, further confirming that autophagy was impaired in these mice. There was also an increased frequency of abnormally swollen mitochondria and mitochondria with decreased cristae density in the *Lamp-2* KO hearts, indicating poor overall mitochondrial health (Fig. 5B, C, G, H). Similar to our *in vitro* results (Fig. 1I, J, Fig. 3B, C), we observed an increased number of mitochondria contained within double membrane AVs (Fig. 5D, I) and a greater degree of mitochondrial fragmentation (Fig. 5B, G) in the hearts of *Lamp-2* KO mice compared to WT littermates, suggesting an impaired clearance of damaged mitochondria. Interestingly, *Lamp-2* KO mice showed normal body weights up to the age of 30 weeks (Table 1, Supplemental Fig. 3A); and despite increases in cardiomyocyte size (Supplemental Fig. 4A–C) and left ventricular wall thickness (Fig. 5A, B), their heart functions were not yet compromised at this age (Table 1, Table 2, Supplemental Fig. 5C); yet aberrant mitochondrial morphology was clearly evident at this early stage of disease development. We decided to evaluate the clearance of these damaged mitochondria by assessing mitophagy. To do so, we isolated mitochondria from the hearts of 20-week old WT and *Lamp-2* KO littermates and assessed for co-localization of the mitophagy regulators Parkin and p62. We observed a significant increase in the expression of Parkin and p62 in the mitochondrial fraction of *Lamp-2* KO hearts compared to WT littermate controls (Fig. 5E, J) indicating increased mitochondrial damage in *Lamp-2* KO hearts. Additionally, LC3-II which is a critical component of the autophagosomal membrane was also increased in the mitochondrial fraction, indicating that mitochondria were more likely to be associated with autophagosomes in *Lamp-2* KO hearts compared to WT (Fig. 5E, J) which further supports our EM findings (Fig. 5D, I). Furthermore, we generated another novel reporter mouse model by crossing *Lamp-2* KO mice with a previously established mt-Kiema mouse line [19]. Using this reporter mouse line, mitophagy can be monitored *in vivo*. The mitochondrial-targeted form of the fluorescent reporter Keima (mt-Keima) has a pH-dependent excitation. Accordingly, the mt-Keima fluorescence signal from mitochondria in the neutral-pH cytoplasmic compartment is green (Keima mitochondria; Supplemental Fig. 6A, B) and the fluorescence signal from mitochondria in the acidic-pH lysosomal compartment is red (Keima autolysosome, Supplemental Fig. 6A′, B′). When the level of mitophagy was assessed by counting the number of red puncta in the cardiomyocytes of *Lamp-2* KO and WT 20-week old littermates, we observed that the delivery

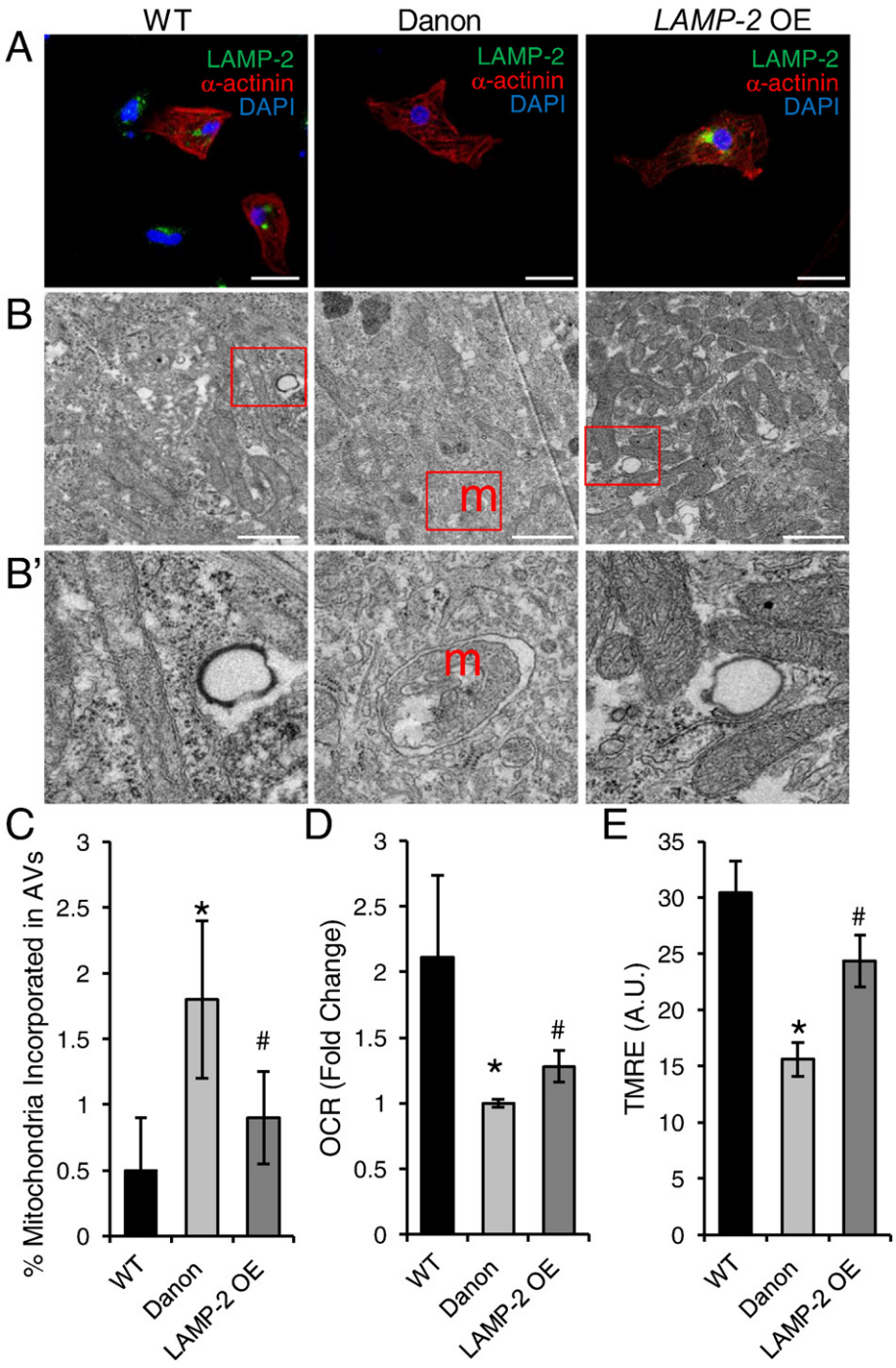

Fig. 3. Re-introduction of *LAMP-2B* in Danon hiPSC-CMs restores mitophagy and rescues mitochondria function and health. (A) Representative confocal images of WT, Danon, and *LAMP-2* overexpression (*LAMP-2* OE) hiPSC-CMs immunostained for sarcomeric α-actinin (red) and LAMP-2 (green) reveal no visible LAMP-2 expression in Danon hiPSC-CMs, and restoration of punctate LAMP-2 expression in *LAMP-2* OE hiPSC-CMs. DAPI (blue) was used to counterstain nuclei. Scale bar = 20 μm. (B) Representative electron microscopy (EM) images of WT, Danon, and *LAMP-2* OE hiPSC-CMs reveal the presence of intact mitochondria within autophagic vacuoles (AVs) in Danon hiPSC-CMs. A reduction in the number of mitochondria incorporated within AVs, and the presence of elongated mitochondria are noted in *LAMP-2* OE hiPSC-CMs compared to Danon hiPSC-CMs. M: Mitochondria. Scale bar = 0.5 μm. (B′) Enlarged images of the boxed areas in B. (C) Quantification of the percentages of mitochondria incorporated in AVs visualized by EM reveals increased percentages in Danon hiPSC-CMs compared to WT and *LAMP-2* OE hiPSC-CMs. (D) Fold change in maximal uncoupler-stimulated oxygen consumption rates (OCR) in intact hiPSC-CMs reveal rescue of respiratory rates in *LAMP-2* OE hiPSC-CMs compared to Danon hiPSC-CMs. (E) hiPSC-CMs from Danon lines show decreased TMRE fluorescence levels compared to WT and *LAMP-2* OE lines. AU: arbitrary units. Student's *t*-test and two-way ANOVA with non-parametric correction followed by post-hoc Dunnett's test, n = 4, $^{*}p < 0.05$ *vs.* WT hiPSC-CMs, $^{\#}p < 0.05$ *vs.* Danon hiPSC-CMs untreated control.

of mitochondria to the lysosomal compartment was significantly low in *Lamp-2* KO cardiomyocytes compared to WT (Supplement Fig. 6C, D). Taken together, these results indicate that *Lamp-2* KO cardiomyocytes exhibit impaired delivery of damaged mitochondria to the lysosomes for degradation, and increased accumulation of damaged mitochondria in both the cytoplasm and within AVs, confirming our *in vitro* findings.

3.6. Lamp-2 KO mouse hearts exhibit reduced mitochondrial respiratory capacity

To determine the effect of impaired mitophagic flux on mitochondrial function *in vivo*, we then assessed mitochondrial respiration by freshly isolated whole heart mitochondria from *Lamp-2* KO and WT

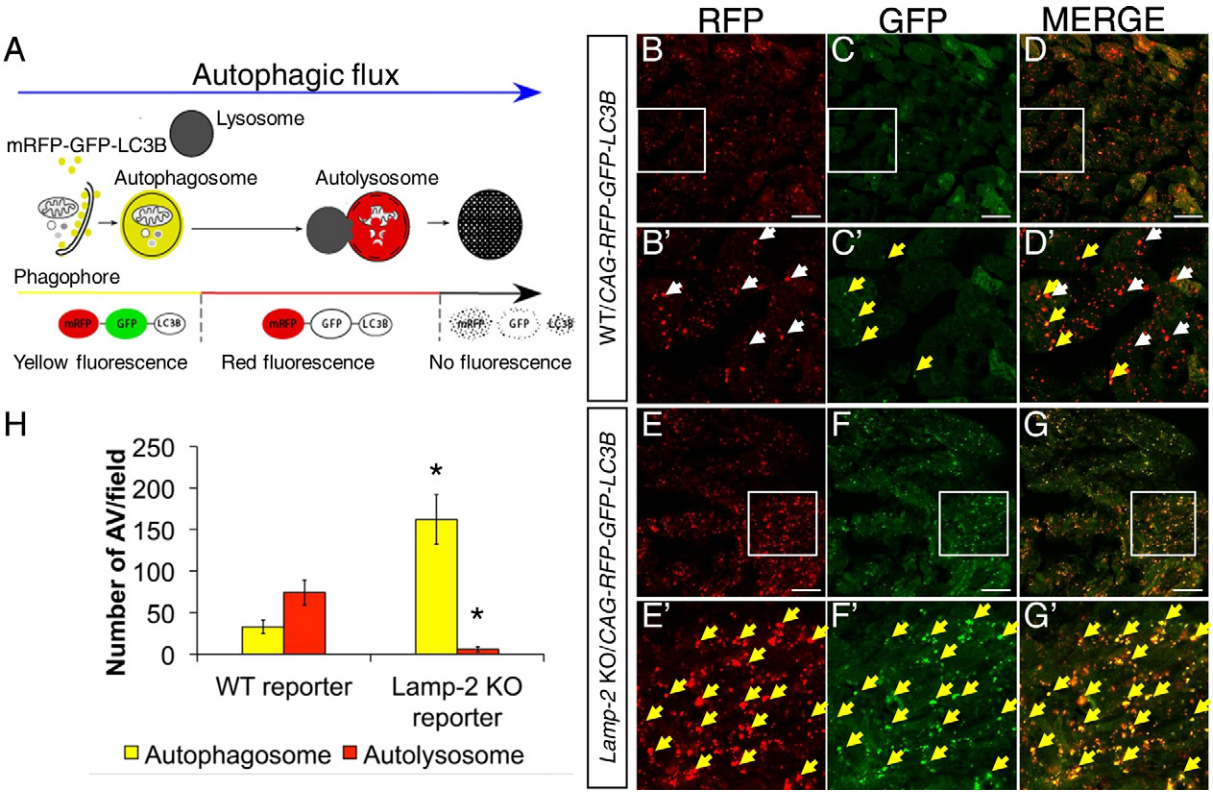

Fig. 4. *Lamp-2* KO/*CAG-RFP-EGFP-LC3B* mice exhibit impaired flux. (A) A schematic of the RFP-EGFP-LC3B reporter system. Autophagosomes are lined by LC3 protein and express both RFP and GFP, so they appear yellow. LAMP-2 is required for the fusion of autophagosomes to lysosomes in order to form autolysosomes. When autophagosomes and lysosomes fuse (*i.e.* autolysosome), GFP is quenched by the acidic pH of lysosomes and only RFP is expressed. Autolysosomes are red only. Modified with permission (Hansen TE, Johansen T. Following autophagy step-by-step. BMC Biology. 2011;9:39). (B–D) Representative confocal images of a WT reporter mouse heart showing (B) RFP and (C) GFP puncta, and (D) merge of the two channels. Note, both red (autolysosomes) and yellow (autophagosomes) exist in this heart. (B′–D′) Enlarged images of the boxed area in B–D. (E–G) Representative confocal images of a *Lamp-2* KO reporter mouse heart showing (E) RFP and (F) GFP puncta, and (G) merge of the two channels. Note, only yellow (autophagosomes) exist in this heart. (E′–G′) Enlarged images of the boxed area in E–G (white arrows: autolysosomes; yellow arrows: autophagosomes). (H) Quantification of autophagic vacuoles (AV): autophagosome (GFP + RFP = yellow) and autolysosome (RFP only) puncta in WT and *Lamp-2* KO 9 week-old mice (AV count is 33 ± 17 and 74 ± 23 for WT, and 162 ± 58 and 6 ± 4 for *Lamp-2* KO, autophagosomes and autolysosomes respectively). Student's *t*-test, n = 4, *p < 0.001 *vs.* WT. Scale bar = 40 μm.

littermates [20]. Previous echocardiographic studies have reported decreased systolic function in *Lamp-2* KO mice [11,21]. Accordingly, we selected to assess mitochondrial function in mice around 32 weeks of age and before the development of overt heart dysfunction, as previously reported [11,21]. Around 32 weeks of age, *Lamp-2* KO mice exhibited early signs of cardiac remodeling on magnetic resonance imaging (MRI) (Table 1) and by echocardiography (Supplemental Fig. 5A, B), however there was no decline in gross contractile functions in these mice as assessed by normal fractional shortening (Supplemental Fig. 5C) and ejection fractions (Table 1). Additionally, invasive hemodynamic studies on *Lamp-2* KO mice at 31–33 weeks of age confirmed the lack of a significant decline in gross cardiac functions (Table 2). However, when individual cardiomyocyte function was evaluated using previously described techniques (IonOptix, fura-2) for single-cell physiologic analysis [22], cardiomyocytes from *Lamp-2* KO hearts demonstrated a decline in calcium transient amplitude (Supplemental Fig. 7A) and decreased sarcomere shortening (Supplemental Fig. 7B) across multiple pacing frequencies when compared to WT littermate controls, indicating a decline in functions at the cellular level at this stage. In Fig. 6A, we show a representative tracing of respiration by isolated mitochondria from these 32-week old mice. The initial rate is in the presence of ADP (State 3 respiration), followed by addition of the ATP synthase inhibitor oligomycin to obtain State 4 rates. Finally, with sequential additions of FCCP maximal uncoupler-stimulated rates were obtained. Mitochondria from *Lamp-2* KO hearts had lower rates of State 3 (ADP-stimulated) and maximal uncoupler-stimulated respiration (Fig. 6A) than WT controls when oxidizing either pyruvate (plus malate) or succinate (with rotenone) (Fig. 6A, B). Rates of mitochondrial oxidation of palmitoyl carnitine (plus malate) were similar between the two genotypes (Fig. 6A, B). The rates of respiration on this substrate were far lower than others (Fig. 6A). This suggests limitation of the rate of respiration at a step of palmitoyl carnitine oxidation that is proximal in the metabolic pathway to the electron transport chain. This rate limitation appears to control the maximal respiratory rate on palmitoyl carnitine in mitochondria from both genotypes. Thus, when respiratory rates are relatively low, a defect in respiration is not evident in *Lamp-2* KO mitochondria, but when respiratory rates are high, as in the presence of pyruvate or succinate as substrate, a defect is readily evident. This data suggests that a global decrease exists in the capacity of the electron transport chain to function in mitochondria of *Lamp-2* KO hearts that would likely lead to tissue dysfunction under high energetic demand. Taken together, these results indicate that the decline in mitochondrial bioenergetic functions proceeds the development of gross cardiac dysfunction in a mouse model of Danon disease.

4. Discussion

Though impaired autophagy has been implicated in the pathophysiology of many cardiovascular disorders the precise mechanisms by which disruptions in autophagic flux lead to cardiac dysfunction remain unresolved. In this study, we investigated the ramifications of impaired autophagy using *in vitro* and *in vivo* models of LAMP-2 deficiency. In both systems, we discovered profound abnormalities in mitophagic flux and mitochondrial function.

In Danon hiPSC-CMs, the initiation of mitophagy was enhanced, based on increased translocation of PARKIN, p62, and LC3-II to the

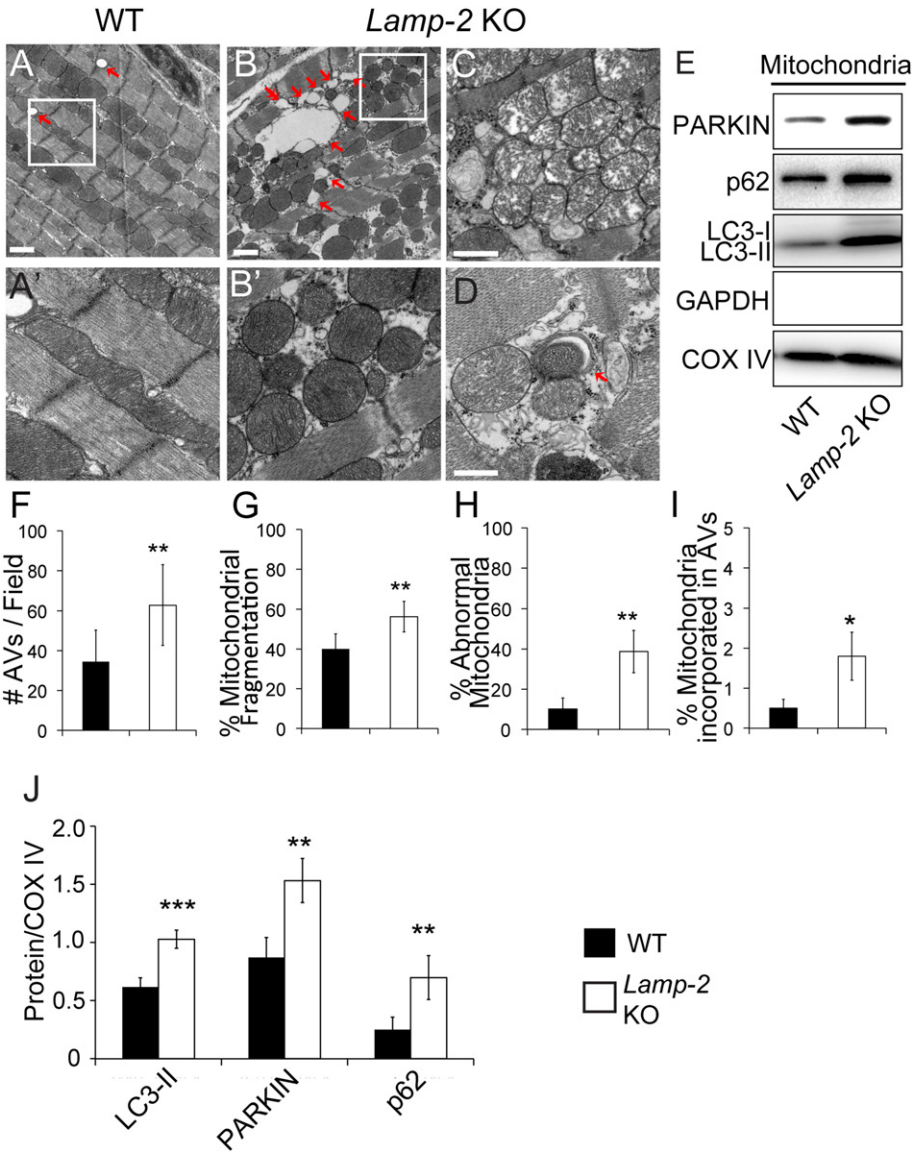

Fig. 5. *Lamp-2* KO mouse hearts exhibit increased mitochondrial morphological abnormalities and impaired mitophagy. (A–D) Representative EM images from 22 week-old (A) WT and (B–D) *Lamp-2* KO hearts show (B) increased mitochondrial fragmentation, (C) abnormal mitochondria with decreased cristae density, and (D) intact mitochondria within autophagic vacuoles (AVs) in *Lamp-2* KO hearts. Scale bar = 0.5 μm. (A′, B′) Enlarged images of boxed area in A, B. (E) Western blots (WB) of LC3-II, Parkin, and p62 in the mitochondrial fractions isolated from WT and *Lamp-2* KO hearts of 22 week-old mice demonstrate increased expression of LC3-II, Parkin, and p62 in isolated mitochondria from *Lamp-2* KO hearts. (F–I) Quantification of AVs (F), percentage of fragmented mitochondria (G), percentage of abnormal (fragmented, swollen, decreased cristae) mitochondria (H), and percentage of mitochondria incorporated within AVs (I) in *Lamp-2* KO hearts compared to WT controls. (J) Quantification of WBs of Parkin, p62 and LC3-II in the mitochondrial fractions isolated from WT and *Lamp-2* KO hearts of 20-week old littermates (0.6 ± 0.07, 0.87 ± 0.17, and 0.25 ± 0.1 for WT *vs.* 1.03 ± 0.078, 1.53 ± 0.19, and 0.7 ± 0.19 for *Lamp-2* KO mice for the expression of LC3-II, Parkin and p62 respectively). COX IV was used as loading control. Student's *t*-test, n = 3–7, *p < 0.05, **p < 0.01, ***p < 0.005. Scale bar = 0.5 μm.

mitochondrial membrane (Fig. 1), likely in response to mitochondrial depolarization (Fig. 1G, H, Fig. 3E, Supplemental Fig. 1). However, an increased number of damaged mitochondria were seen contained within AVs in Danon hiPSC-CMs (Fig. 1J, Fig. 3B, C), indicated that mitophagy could not be completed. These mitochondrial abnormalities were associated with a significant reduction in mitochondrial respiratory capacity

Table 1
Cardiac magnetic resonance imaging data.

	WT	*Lamp-2* KO
BW (g)	33.3 ± 3	31.3 ± 3
Age (weeks)	30.9 ± 2	30.9 ± 2
ED volume (μL)	56.8 ± 6.1	79.3 ± 12.4*
ES volume (μL)	16.7 ± 0.8	28.2 ± 2.4*
EF (%)	70.4 ± 3.8	64.2 ± 5.5
LV mass (mg)	78.9 ± 12.3	91.8 ± 13.7
Number	3	4

Body weight: BW; End-diastole: ED; End-systole: ES; Ejection fraction: EF; Left ventricle: LV. Student's *t*-test.
* p < 0.05 *vs.* WT.

Table 2
Invasive hemodynamic studies data.

	WT	*Lamp-2* KO
Age (weeks)	32 ± 0.7	32.3 ± 0.7
Heart rate (bpm)	346.2 ± 30.6	293.1 ± 81.1
Maximum pressure (mm Hg)	104.5 ± 14.2	91.9 ± 14.6
Minimum dP/dt (mm Hg/s)	−6485.7 ± 1031.3	−5499.7 ± 352.3
Maximum dP/dt (mm Hg/s)	8649.9 ± 1038.4	6562.1 ± 1818*
End-diastolic pressure (mm Hg)	3.5 ± 1	5.6 ± 3.7
Exponential Tau (ms)	12.3 ± 0.6	13.7 ± 3.4
Number	7	7

Student's *t*-test.
* p < 0.05 *vs.* WT.

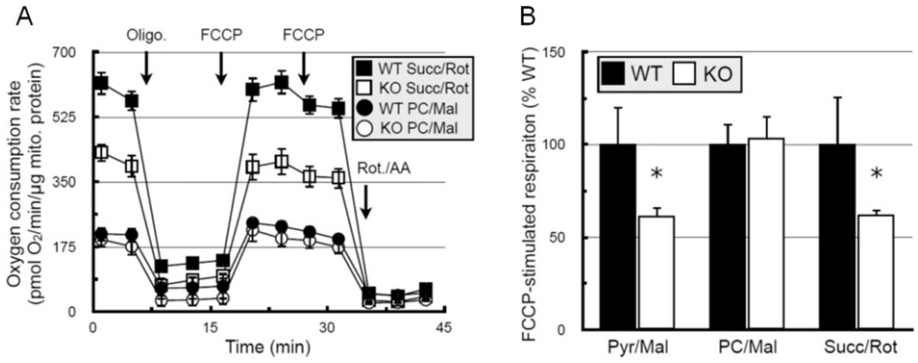

Fig. 6. *Lamp-2* KO mouse hearts exhibit increased mitochondrial damage and altered mitochondrial respiratory capacity. (A) Representative tracing of oxygen consumption rate (OCR) measurement in mitochondria freshly isolated from WT and *Lamp-2* KO mouse hearts at age 32 weeks with palmitoyl carnitine plus malate (PC/Mal) or succinate plus rotenone (Succ/Rot) provided as a substrate. Sequential additions as indicated are 1 μM oligomycin (oligo), 1 μM carbonyl cyanide-4-(trifluoromethoxy) phenylhydrazone (FCCP), then 0.5 μM rotenone plus 1 μM antimycin A (Rot./AA). (B) The mean OCR in mitochondria from WT and *Lamp-2* KO hearts with pyruvate plus malate (Pyr/Mal), PC/Mal, or Succ/Rot provided as substrates normalized to the rates in WT mitochondria reveal decreased OCR levels in *Lamp-2* KO mitochondria on Pyr/mal and Succ/Rot. n = 4 with 8–10 biologic replicates per mitochondrial preparation. Two-way ANOVA with non-parametric correction followed by post-hoc Dunnett's test, $^{*}p < 0.05$, *vs.* WT.

(Fig. 2A–C). We previously reported that Danon hiPSC-CMs exhibit increased mitochondrial oxidative stress [10]. Our current findings provide insight into the mechanisms leading to increased mitochondrial oxidative stress and apoptosis in LAMP-2 deficient cardiomyocytes. Our results suggest that impaired clearance of damaged mitochondria results in the accumulation of damaged mitochondria within AVs that then become a source of ROS-induced-ROS release leading subsequently to cardiomyocyte dysfunction and death. This conclusion is further supported by the rescue in mitophagy and mitochondrial function observed following the re-introduction of *LAMP-2B* in Danon hiPSC-CMs (Fig. 3). As LAMP-2B principally regulates macroautophagy, these finding suggests that interventions targeted toward this specific pathway should be sufficient to improve metabolic function in Danon disease. It also suggests that such interventions may be of use in other conditions associated with impaired autophagic flux. We have previously shown that *LAMP-2B* overexpression decreased the levels of mitochondrial ROS in Danon hiPSC-CMs [10]. Here, we show that the re-introduction *LAMP-2B* rescued mitophagy, mitochondrial health, and mitochondrial function, providing evidence that proper recycling of damaged 'leaky' mitochondria *via* macroautophagy is essential for cardiomyocyte health (Supplemental Fig. 8). The relatively modest yet significant rescue of OCR in the *LAMP-2* OE hiPSC-CM line (Fig. 3D) might be due to the persistence of other cellular abnormalities resulting from impairment of the other different forms of autophagy (*i.e.* chaperone mediate autophagy and microautophagy), such as the decreased availability of substrates required from proper mitochondrial functioning. Nonetheless, the overexpression of *LAMP-2B* in Danon hiPSC-CMs was sufficient to rescue the compromised mitochondrial membrane potential (Fig. 3E), providing evidence that proper autophagic flux of damaged mitochondria improves overall mitochondrial health.

Because hiPSC-CM models have inherent limitations, such as the relative immaturity of cardiomyocytes [23], we sought to confirm our *in vitro* findings *in vivo* by utilizing a *Lamp-2* KO mouse model of Danon disease [11,21]. *Lamp-2* KO mice had severely impaired autophagic flux with disrupted autophagosome-lysosome fusion as assayed by a *CAG-RFP-EGFP-LC3B* reporter system (Fig. 4). Cardiomyocytes from *Lamp-2* deficient mice also demonstrated evidence of incomplete mitophagic flux (Fig. 5D, I, E, J) and decreased mitochondrial respiratory function (Fig. 6). Using a novel mt-Keima reporter mouse line, we were able to monitor mitophagy in *Lamp-2* KO cardiomyocytes (Supplemental Fig. 6). Despite the limitations of *ex vivo* analysis of isolated cardiomyocytes, we chose this method due to the higher resolution it offers for analyzing fluorescence per cardiomyocyte. Our results show that *Lamp-2* KO cardiomyocytes exhibited a significant decrease in basal delivery of mitochondria to the acidic lysosomal compartments compared to WT, and provide evidence of the presence of non-conventional mitophagy pathways albeit at a less efficient level than the canonical mitophagy pathway (*i.e.* autophagosome-lysosome fusion pathway). These observations were completely consistent with our findings in Danon hiPSC-CMs.

Physiologically, *Lamp-2* KO mice exhibited early signs of cardiac remodeling on MRI and echocardiography (Table 1, Supplemental Fig. 5A, B) as well as evidence of contractile dysfunction at the cellular level (Supplemental Fig. 7); however they showed no evidence of gross cardiac dysfunctions as assessed by normal fractional shortening (Supplemental Fig. 5C) and ejection fraction levels (Table 1) at the age when mitochondrial bioenergetics were assessed (Fig. 6). Previous studies have shown that *Lamp-2* KO mice have increased ROS levels as evident by increased levels of ROS-modified (carbonylated) proteins in cardiac extracts from young *Lamp-2* KO [24]. Thus, it appears that the oxidative stress, and mitochondrial and metabolic abnormalities caused by loss of LAMP-2 expression occur before the development of end-stage heart failure in the mouse model of Danon disease (Supplemental Fig. 8). This is consistent with the clinical course of Danon disease in humans, in which evidence of cardiac hypertrophy and mild cardiac dysfunction precede the development of overt clinical heart failure by many years [25]. Our observations here suggest that early interventions to correct the underlying metabolic abnormalities caused by LAMP-2 deficiency may prevent Danon disease patients from progressing to end-stage heart failure.

5. Conclusion

Studying patient-derived hiPSC-CMs in combination with robust animal models has the potential to greatly improve our understanding of the pathophysiology of inherited diseases and to develop treatments for those diseases. Here, we show that mitochondrial damage/dysfunction and incomplete mitophagy are key pathophysiological mechanisms through which disruption of macroautophagy causes cardiomyocyte dysfunction using both *in vitro* and *in vivo* models of Danon disease. These findings suggest that therapies targeted at improving mitochondrial health and autophagic flux may serve as effective treatments for this highly morbid disorder, which currently has no specific therapeutic options, as well as other cardiovascular diseases associated with impaired autophagy.

Funding

This research was funded by grants from the National Institutes of Health, the California Institute of Regenerative Medicine (CIRM), and the American Heart Association (AHA): 7K23HL107755 and CIRM TR305687 for E.D.A., and NS087611 and a gift from Seahorse

Bioscience/Agilent Technologies to A.N.M., and postdoctoral fellowship AHA grant 16POST29740010 for S.I.H.

Conflict of interest

The authors have no conflicts of interest to disclose.

Disclosures

None.

Acknowledgements

We thank members of the Adler and Chi lab for their support and intellectual and editorial feedback during this project. We thank Matthieu Bauer (UCSD) for assistance with stem cell maintenance, and Jan Schilling and Hamel Patel (UCSD) for assistance with the initial mitochondrial studies. We also thank the UCSD CMM EM facility for preparation of EM slides, Dr. Paul Saftig (University of Kiel, Germany) for the *Lamp-2* KO mice, and Dr. Joseph Hill (University of Texas Southwestern) for the *CAG-RFP-EGFP-LC3B* reporter mice.

Appendix A. Supplementary data

Supplementary data to this article can be found online at http://dx.doi.org/10.1016/j.yjmcc.2017.05.007.

References

[1] Y. Endo, A. Furuta, I. Nishino, Danon disease: a phenotypic expression of LAMP-2 deficiency, Acta Neuropathol. 129 (2015) 391–398.
[2] B.J. Maron, W.C. Roberts, M. Arad, T.S. Haas, P. Spirito, G.B. Wright, et al., Clinical outcome and phenotypic expression in LAMP2 cardiomyopathy, JAMA 301 (2009) 1253–1259.
[3] I. Nishino, J. Fu, K. Tanji, T. Yamada, S. Shimojo, T. Koori, et al., Primary LAMP-2 deficiency causes X-linked vacuolar cardiomyopathy and myopathy (Danon disease), Nature 406 (2000) 906–910.
[4] E.L. Eskelinen, Y. Tanaka, P. Saftig, At the acidic edge: emerging functions for lysosomal membrane proteins, Trends Cell Biol. 13 (2003) 137–145.
[5] E.L. Eskelinen, A.L. Illert, Y. Tanaka, G. Schwarzmann, J. Blanz, K. Von Figura, et al., Role of LAMP-2 in lysosome biogenesis and autophagy, Mol. Biol. Cell 13 (2002) 3355–3368.
[6] D.S. Konecki, K. Foetisch, K.P. Zimmer, M. Schlotter, U. Lichter-Konecki, An alternatively spliced form of the human lysosome-associated membrane protein-2 gene is expressed in a tissue-specific manner, Biochem. Biophys. Res. Commun. 215 (1995) 757–767.
[7] Z. Li, J. Wang, X. Yang, Functions of autophagy in pathological cardiac hypertrophy, Int. J. Biol. Sci. 11 (2015) 672–678.
[8] B.J. Sishi, B. Loos, J. van Rooyen, A.M. Engelbrecht, Autophagy upregulation promotes survival and attenuates doxorubicin-induced cardiotoxicity, Biochem. Pharmacol. 85 (2013) 124–134.
[9] X. Wu, L. He, F. Chen, X. He, Y. Cai, G. Zhang, et al., Impaired autophagy contributes to adverse cardiac remodeling in acute myocardial infarction, PLoS One 9 (2014) e112891.
[10] S.I. Hashem, C.N. Perry, M. Bauer, S. Han, S.D. Clegg, K. Ouyang, et al., Oxidative stress mediates cardiomyocyte apoptosis in a human model of Danon disease and heart failure, Stem Cells 33 (2015) 2343–2350.
[11] Y. Tanaka, G. Guhde, A. Suter, E.L. Eskelinen, D. Hartmann, R. Lüllmann-Rauch, et al., Accumulation of autophagic vacuoles and cardiomyopathy in LAMP-2-deficient mice, Nature 406 (2000) 902–906.
[12] X. Lian, J. Zhang, S.M. Azarin, K. Zhu, L.B. Hazeltine, X. Bao, et al., Directed cardiomyocyte differentiation from human pluripotent stem cells by modulating Wnt/β-catenin signaling under fully defined conditions, Nat. Protoc. 8 (2013) 162–175.
[13] A.S. Divakaruni, A. Paradyse, D.A. Ferrick, A.N. Murphy, M. Jastroch, Analysis and interpretation of microplate-based oxygen consumption and pH data, Methods Enzymol. 547 (2014) 309–354.
[14] G. Ashrafi, T.L. Schwarz, The pathways of mitophagy for quality control and clearance of mitochondria, Cell Death Differ. 20 (2013) 31–42.
[15] I. Kim, S. Rodriguez-Enriquez, J.J. Lemasters, Selective degradation of mitochondria by mitophagy, Arch. Biochem. Biophys. 462 (2007) 245–253.
[16] D.A. Kubli, A.B. Gustafsson, Mitochondria and mitophagy: the yin and yang of cell death control, Circ. Res. 111 (2012) 1208–1221.
[17] N.C. Chan, A.M. Salazar, A.H. Pham, M.J. Sweredoski, N.J. Kolawa, R.L. Graham, et al., Broad activation of the ubiquitin-proteasome system by Parkin is critical for mitophagy, Hum. Mol. Genet. 20 (2011) 1726–1737.
[18] L. Li, Z.V. Wang, J.A. Hill, F. Lin, New autophagy reporter mice reveal dynamics of proximal tubular autophagy, J. Am. Soc. Nephrol. 25 (2014) 305–315.
[19] N. Sun, J. Yun, J. Liu, D. Malide, C. Liu, I.I. Rovira, et al., Measuring in vivo mitophagy, Mol. Cell 60 (2015) 685–696.
[20] G.W. Rogers, M.D. Brand, S. Petrosyan, D. Ashok, A.A. Elorza, D.A. Ferrick, et al., High throughput microplate respiratory measurements using minimal quantities of isolated mitochondria, PLoS One 6 (2011) e21746.
[21] J. Stypmann, P.M. Janssen, J. Prestle, M.A. Engelen, H. Kögler, R. Lüllmann-Rauch, et al., LAMP-2 deficient mice show depressed cardiac contractile function without significant changes in calcium handling, Basic Res. Cardiol. 101 (2006) 281–291.
[22] T.J. Herron, E. Devaney, L. Mundada, E. Arden, S. Day, G. Guerrero-Serna, et al., Ca^{2+}-independent positive molecular inotropy for failing rabbit and human cardiac muscle by alpha-myosin motor gene transfer, FASEB J. 24 (2010) 415–424.
[23] J.J. Savla, B.C. Nelson, C.N. Perry, E.D. Adler, Induced pluripotent stem cells for the study of cardiovascular disease, J. Am. Coll. Cardiol. 64 (2014) 512–519.
[24] R.J. Godar, X. Ma, H. Liu, J.T. Murphy, C.J. Weinheimer, A. Kovacs, et al., Repetitive stimulation of autophagy-lysosome machinery by intermittent fasting preconditions the myocardium to ischemia-reperfusion injury, Autophagy 11 (2015) 1537–1560.
[25] R.S. D'souza, C. Levandowski, D. Slavov, S.L. Graw, L.A. Allen, E. Adler, et al., Danon disease: clinical features, evaluation, and management, Circ. Heart Fail. 7 (2014) 843–849.